文章编号：1001-9014(2022)03-0540-05

DOI:10.11972/j.issn.1001-9014.2022.03.003

Tunable dual-wavelength semiconductor laser based on indium-rich cluster quantum structure

LI Xue[1,2], TAI Han-Xu[3], WANG Yu-Hong[3], ZHENG Ming[3], ZHANG Jian-Wei[1], ZHANG Xing[1*], NING Yong-Qiang[1], WU Jian[3], WANG Li-Jun[1]

(1. State Key Laboratory of Luminescence and Application, Changchun Institute of Optics, Fine Mechanics and Physics, Chinese Academy of Sciences, Changchun 130033, China;
2. Center of Materials Science and Optoelectronics Engineering, University of Chinese Academy of Sciences, Beijing 100049, China;
3. School of Physics, Beihang University, Beijing 100191, China)

Abstract: We design and fabricate a double-wavelength tunable laser with a single grating structure using a single-gain chip. The gain chip adopts an indium-rich cluster quantum constraint structure, which can generate ultra-wide flat-top gain. The flat-top gain is the basis for producing a dual-wavelength laser with the same intensity. A grating is inserted into the exterior of the gain chip so that its resonator is composed of internal and external cavities. The internal cavity consists of two natural cleavage planes of the gain chip for oscillating the output laser at a fixed wavelength (974 nm). The tunable external cavity consists of a natural cleavage plane and a grating for the output laser at a tunable wavelength (969.1~977.9 nm). The laser structures of the single-gain chip and single grating can produce synchronous dual-wavelength output, which avoids a complicated optical path design. The frequency difference between the two wavelengths is in the terahertz band. Thus, the laser can be used as a dual-wavelength laser source to generate terahertz radiation.

Key words: tunable laser, dual-wavelength laser, indium-rich clusters

基于富铟团簇量子结构的双波长可调谐半导体激光器

李 雪[1,2], 邰舍旭[3], 王玉龙[3], 郑 明[3], 张建伟[1], 张 星[1*], 宁永强[1], 吴 坚[3], 王立军[1]

(1. 中国科学院长春光学精密机械与物理研究所 发光学及应用国家重点实验室,吉林 长春 130033;
2. 中国科学院大学 材料与光电研究中心,北京 100049;
3. 北京航空航天大学,北京 100191)

摘要:提出了一种采用增益芯片和光栅外腔的双波长可调谐半导体激光器。增益芯片采用了富铟团簇量子限制结构作为其量子限制结构,由于该结构独特的平顶增益特性,可以使激光器在双波长调谐范围内实现光强稳定。本研究中的谐振腔包括内部谐振腔和外部谐振腔,其中内部谐振腔由增益芯片的两个自然解理面构成,以支撑整个系统工作在特定波长。外部谐振腔由增益芯片的一个自然解理面和光栅构成,可实现969.1~977.9 nm的工作波长范围。最终该系统基于单个增益芯片和单个光栅实现了同步双波长输出,双波长的频率差在THz范围。本研究有望为实现双波长差频太赫兹源提供一种可能的解决方案。

关 键 词:半导体激光器;富铟团簇;可调谐

中图分类号:TN248.4　　**文献标识码**:A

Received date: 2021-10-01, **revised date**: 2021-11-18　　**收稿日期**:2021-10-01,**修回日期**:2021-11-18

Foundation items: Supported in part by the National Key Research and Development Program (2020YFC2200300), in part by the National Natural Science Foundation of China (11774343, 51672264, 61874119, 61874117), in part by the Science and Technology Development Project of Jilin Province (20200401006GX).

Biography: Li Xue (1992-), female, Tonghua, Ph. D. candidate. Research field is semiconductor laser design and fabrication. E-mail: 994099959@qq.com

[*] **Corresponding author**: E-mail: zhangx@ciomp.ac.cn

Tunable dual-wavelength lasers have been widely studied for their applications in distance measurement[1], imaging systems[2], spectral analysis[3], and terahertz wave generation[4-6]. Various methods and structures have been reported to achieve a tunable synchronous dual-wavelength operation. A common structure uses a V-shaped external cavity to select the wavelength by adjusting the spacing of V-shaped slits[7-9]. Another structure uses two gratings to construct two external cavities, and each external cavity corresponds to one lasing wavelength[10-12]. Alternatively, two separate gain chips are used and a birefringent filter is used to tune both wavelengths simultaneously[13]. Other methods include using a Fabry - Perot cavity and a Brewster window[14]. The aforementioned methods are limited in practical application and integration because they require coating or using an excessive number of optical elements. Therefore, an essential problem to be solved is how to simplify the structure of the dual-wavelength laser and keep the output power of the two different wavelengths roughly equal in the tuning process. In fact, the internal and external cavity coupling can simplify the laser structure. However, in traditional quantum-based structures, achieving synchronous dual-wavelength lasing is difficult because of carrier recombination competition in sub-bands.

In this study, we introduce a method to obtain tunable dual wavelength using a single-gain chip and single grating structure. In this dual-wavelength laser system, InGaAs quantum well with an indium-rich cluster (IRC) quantum limited structure is used as the gain medium. The two laser wavelengths are generated by the oscillations of the two resonators. A stable single wavelength at 974.1 nm was obtained through the internal cavity (two natural cleavage surfaces). The external cavity formed by the blazed grating and natural cleavage surface is used to tune the resonance wavelength of another tuning range of 9 nm. Based on the design of internal and external cavity coupling, the tunable frequency difference between the double wavelength is determined, and the maximum spectrum separation is 4.9 nm. Fig. 1 shows the structure of a dual-wavelength laser coupled with internal and external cavities.

For semiconductor lasers, the gain characteristics of the active region greatly affect their laser characteristics. In this study, the gain medium used in the tunable dual wavelength laser is an InGaAs quantum confinement structure with IRC effect. The $In_{0.17}Ga_{0.83}As/GaAs/GaAs_{0.92}P_{0.08}$ material system is used as the active layer for the gain chip. The thickness of the $In_{0.17}Ga_{0.83}As$ quantum well layer is 10 nm. The quantum well layer with thickness beyond the critical level is grown to obtain enough strain accumulation to generate the IRC effect[15]. Owing to the lattice mismatch between the active and barrier layers, the indium atoms in the quantum well layer migrate in the growth direction due to the large strain during material growth. The growth temperature of the material is set at 660 ℃, and a higher growth temperature can increase the migration length of indium atoms. Under the stress and high temperature, indium atoms migrate to the surface of $In_{0.17}Ga_{0.83}As$ quantum well layer during the growth process, forming numerous indium-rich clusters. At the same time, the migration of indium atoms results in the loss of indium content in the corresponding InGaAs region, forming several discrete $In_xGa_{1-x}As$ active regions with different indium contents. The superposition of these active regions with different indium components results in the special flat-top gain characteristics of this structure. The barrier layer is $GaAs_{0.92}P_{0.08}$ with 8 nm thickness. A 2 nm thick GaAs strain compensation layer exists between the quantum well and barrier layers, and the IRCs formed on the surface of InGaAs are observed by atomic force microscope (AFM), as shown in Fig. 2.

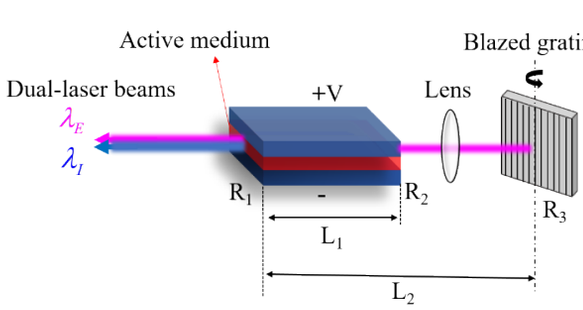

Fig. 1　Schematic of internal and external cavity structures of tunable dual-wavelength laser
图1　可调谐双波长激光器的内腔和外腔结构示意图

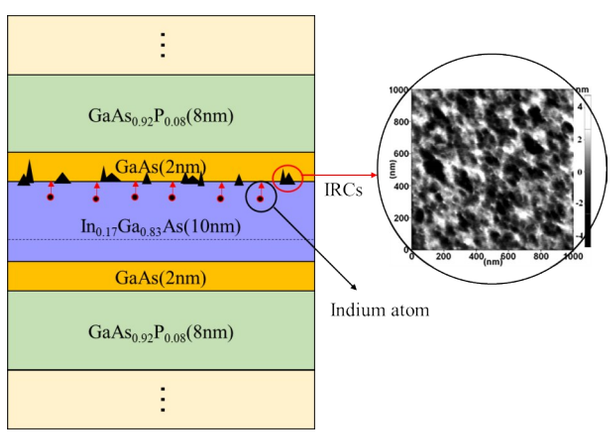

Fig. 2　Structure of sample and AFM photograph of indium-rich clusters
图2　富铟团簇结构的AFM测试结果

Except for the pumping method, the growth conditions and sample structure are consistent with the samples we used previously[15]. The size of the gain chip is 0.5×1.5 mm. No coating is found on both sides of the sample. The aspheric lens (L_1, with a focal length of 4.6 mm, NA = 0.52) (Thorlabs, Newton, New Jersey, USA) was placed on the back end of the sample for collimator beams. The blazed grating (Thorlabs) is 1200 line/mm, with a blazed wavelength of 1000 nm and a diffraction efficiency of 65%. It is placed 60 mm from the rear end of the sample to feed back the resonant beam. In this manner, we obtain two resonant cavities (one internal

and the other external) for producing double-wavelength lasing. To avoid the thermal effect, the samples were placed on a TEC thermoelectric cooler at 273 K.

For the structure shown in Fig. 1, the intra-cavity loss of the laser system is evaluated by the threshold gain analysis. The threshold gains of the internal and external cavities can be expressed, respectively as follows, according to the self-consistency conditions, I_1 and I_2 are the light intensity values of a beam with light intensity I_0 after a round trip in the internal and external cavities, respectively.

$$I_1 = I_0 R_1 R_2 e^{(G-\alpha_i)\cdot 2L_1} \quad , \quad (1)$$

$$I_2 = I_0 R_1 (1-R_2)^2 R_3 e^{(G-\alpha_i)\cdot 2L_1} e^{-\alpha_e \cdot L_2} \quad , \quad (2)$$

where R_1 and R_2 are the reflectivity of the two facets of the laser medium and R_3 is the reflectivity of the grating. G is the modal gain of the medium, α_i is the internal loss factor of the internal cavity, α_e is the transmission loss of the laser in the air, L_1 is the length of the internal cavity, and L_2 is the length from R_2 to R_3. According to equation (1), the threshold gain of the internal cavity can be expressed as equation (3).

$$G_{th} = \alpha_i + \frac{1}{2L_1}\ln\left(\frac{1}{R_1 R_2}\right) \quad . \quad (3)$$

According to equation (2), the threshold gain of the internal cavity can be expressed as equation (4).

$$G_{th} = \alpha_i + \frac{2L_2}{2L_1}\cdot\alpha_e + \frac{1}{2L_1}\ln\left(\frac{1}{R_1(1-R_2)^2 R_3}\right). \quad (4)$$

If R_1=30% and R_3=65% are substituted into equations (3) and (4), then the threshold gain is a function of R_2. Owing to the insertion of R_2, the mode gain of the external cavity increases from 9.4 cm^{-1} to 11.8 cm^{-1}. Moreover, when R_2=30%, the difference between the threshold gain of the internal and external cavities is only 0.2 cm^{-1}, which can almost be stimulated together with the same injection.

In the obtained synchronous dual-wavelength laser, the wavelength of 974 nm is fixed, while the other wavelength is formed by first-order diffraction feedback to the gain medium through oscillations in this medium. This wavelength is related to the rotation angle of the blazed grating, which can be calculated by grating equation. In fact, a tunable external cavity is formed between the blazed grating and the rear end of the gain chip, and the tunable band is distributed at the fixed wavelength of approximately 974 nm. The left end of the fixed wavelength is defined as negative and the right end is positive. Under the condition that the intensity of the dual wavelength is basically the same, a series of tunable wavelengths are obtained, as shown in Fig. 3. Tuning to shortwave at fixed wavelengths yields a wavelength difference up to 4.9 nm, while tuning to longwave yields a wavelength difference up to 3.9 nm. The threshold current is 430 mA without the external cavity and increased to 490 mA with the external cavity. The maximum continuous output power is 18.9 mW.

The amplified spontaneous emission I_{EASE} of the sample with indium-rich cluster structure is experimentally

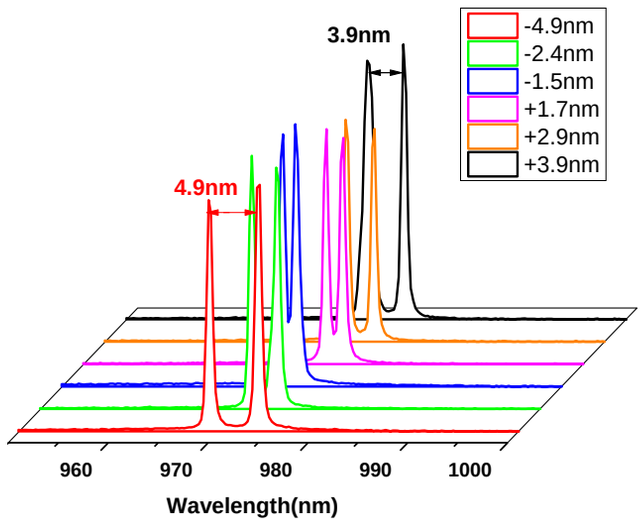

Fig. 3 Fixed wavelength is 974 nm and tuned wavelength is 969.1 – 977.9 nm
图3 固定输出波长为974 nm,可调谐波段为969.1~977.9 nm

compared with the amplified spontaneous emission I_{TASE} of the traditional quantum well calculated theoretically, as shown in Fig. 4. The solid line is the experimental measurement, and the dotted line is the theoretical calculation. The amplified spontaneous radiation of the traditional quantum well is calculated by the theoretical spontaneous radiation intensity and theoretical gain[16]. Fig. 4 shows that, at different carrier injection concentrations, the amplified spontaneous emission of the sample with indium-rich clusters effect is higher and wider than that of the traditional quantum well at the peak, which also determines the range and difficulty of tuning to both ends of the fixed wavelength in the tuning experiment.

The results in Fig. 4 show that the main peak in the experimental ASE spectrum is remarkably broadened and becomes flatter from 969 nm to 978 nm, in comparison

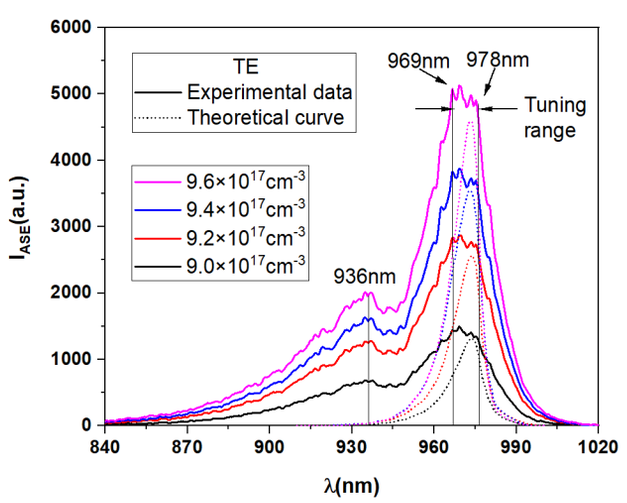

Fig. 4 ASE spectrum obtained by experiment (dashed line) and ASE spectrum obtained by theoretical calculation (solid line)
图4 虚线为实验测试获得的ASE谱,实现为理论计算结果

with the emission peak from the conventional well. The careful observation can find that the main peak actually consists of two sub-peaks of (969 nm) and (978 nm). Hence, this enables synchronous dual-wavelength lasing in the range of 969 nm to 978 nm for the IRC-composite active medium, in terms of the carrier recombination and mode competition effects.

The optical gain can be obtained from the polarization ASE spectra measured on the two end faces of the indium-rich cluster sample [17]. In this method, the ASE spectrum measured in Fig. 4 is taken into the calculation to obtain the gain at different carrier concentrations. The gain fluctuation in 958 nm-992 nm is only 0.8 cm^{-1} with injection current densities of 9.6×10^{17} cm^{-3}.

The analysis on energy-band can interpret the multi-peak feature of the ASE spectrum due to the IRC effect in the $In_xGa_{1-x}As$ active medium. The three peaks of 936 nm, 969 nm and 978 nm in the spectrum are corresponding to the indium contents of x=0.12, 0.15 and 0.17, respectively, which are apparently formed due to the indium atom migration in the IRC effect. Therefore, the energy-band structure of the sample presents the complex and heterogeneous feature. Therefore, the energy-band structure of the sample presents the complex and heterogeneous feature. It is illustrated by Fig. 4. Since the $In_xGa_{1-x}As$ materials with x=0.17 and 0.15 in the active medium present compressive strains, their emissions are inherently in the transverse-electric (TE) polarization mode[18]. The excitation in the internal cavity is a transition from the Fermi level of the conduction band to the Fermi level of the valence band (974 nm). With the addition of the external cavity, the tunable excitation generated by the tunable external cavity can be adjusted on both sides of the Fermi level. However, dual-wavelength laser operation with equal intensity requires an equal number of carriers on its corresponding band. It can only be tuned in the band of 970 – 980 nm. The laser wavelength of the internal cavity is 974 nm. When the carrier is injected into the quantum well, the irregular well formed by the IRC structure stores enough carrier on the sub-energy level of the shortwave segment at 974 nm for the compound laser generation. Thus, the laser intensity produced by the external cavity is not reduced when the external cavity is tuned to the shortwave length.

Two reasons can be cited for using an indium-rich cluster effect quantum-confined structure as a gain chip. First, the unusual quantum-well structure generated by indium-rich cluster effect can effectively solve the carrier competition between sub-bands, thereby forming a stable dual-wavelength lasing operation. Second, comparison with the traditional quantum well shows that the quantum-restricted structure of indium-rich clusters has a certain broadening effect on the gain and spontaneous emission of the sample due to the large number of indium components produced in different regions. Furthermore, the tunable external cavity has certain advantages in tuning to both ends of the fixed wavelength.

We further investigate differential crystals suitable for 974 nm bands and other mixing methods to obtain tunable terahertz radiation from dual-wavelength lasers with wavelength differences[19].

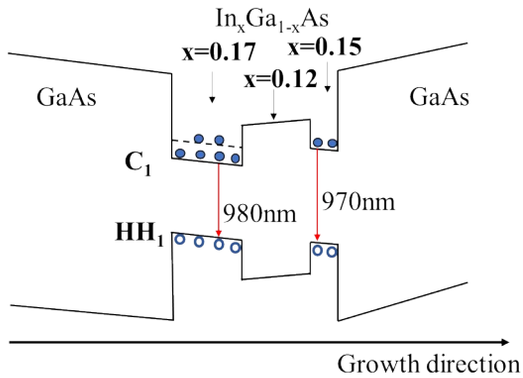

Fig. 5　Special energy band structure in quantum-confined structure of indium-rich clusters
图5　富铟团簇量子限制结构的特殊能带结构

In conclusion, according to the characteristics of IRC structure samples, a synchronous tunable dual-wavelength laser was designed using a single chip and a single grating, which greatly simplified the structure of the tunable dual-wavelength laser and obtained 974 nm/ (969.1 – 977.9 nm) synchronous dual-wavelength lasing operation. At the same time, the advantages of the IRC structure in a tunable dual wavelength laser are proved.

References

[1] WAN Hong-Lin, CAI Wei, WANG Fei, *et al*. High-quality monolayer graphene for bulk laser mode-locking near 2 μm [J]. *Optical and Quantum Electronics*, 2016, **48**(1).
[2] SIEBERT K, QUAST H, LEONHARDT R, *et al*. Continuous-wave all-optoelectronic terahertz imaging [J]. *Applied Physics Letters*, 2002, **80**(16): 3003-3005.
[3] JAGERSKA J, JOUY P, HUGI A, *et al*. Dual-wavelength quantum cascade laser for trace gas spectroscopy [J]. *Applied Physics Letters*, 2014, **105**(16).
[4] SASAKI Y, YOKOYAMA H, ITO H, *et al*. Dual-wavelength optical-pulse source based on diode lasers for high-repetition-rate, narrow-bandwidth terahertz-wave generation [J]. *Optics Express*, 2004, **12**(14): 3066-3071.
[5] YANG S, WATTS R T, LI X, *et al*. Tunable terahertz wave generation through a bimodal laser diode and plasmonic photomixer [J]. *Optics Express*, 2015, **23**(24): 31206-31215.
[6] MEI Jia-Lin, ZHONG Kai, WANG Mao-Rong, *et al*. Widely-tunable high-repetition-rate terahertz generation in GaSe with a compact dual-wavelength KTP OPO around 2 μm [J]. *Optics Express*, 2016, **24**(20): 23368-23375.
[7] LIN C F, CHEN M J, LEE B L. Wide-range tunable dual-wavelength semiconductor laser using asymmetric dual quantum wells [J]. *IEEE Photonics Technology Letters*, 1998, **10**(9): 1208-1210.
[8] GU P, CHANG F, TANI M, *et al*. Generation of coherent cw-terahertz radiation using a tunable dual-wavelength external cavity laser diode [J]. *Japanese Journal of Applied Physics*, 1999, **38**(11): 1246-1248.
[9] HOFFMANN S, HOFMANN M R, KIRA M, *et al*. Two-colour diode lasers for generation of THz radiation [J]. *Semiconductor Science and Technology*, 2005, **20**(7).
[10] ZOLOTOVSKAYA S, DAGHESTANI N S, VENUS G, *et al*. Stable dual-wavelength operation of InGaAs diode lasers with volume Bragg gratings [J]. *Applied Physics Letters*, 2007, **91**(17).
[11] CHI M, JENSEN O B, PETERSEN P M, *et al*. High-power dual-wavelength external-cavity diode laser based on tapered amplifier with tunable terahertz frequency difference [J]. *Optics Letters*, 2011, **36**(14): 2626-2628.

[12] ZHENG Y, KURITA T, SEKINE T, *et al*. Tunable continuous-wave dual-wavelength laser by external-cavity superluminescent diode with a volume Bragg grating and a diffraction grating [J]. *Applied Physics Letters*, 2016, **109**(14).
[13] ZHU Ren-Jiang, WANG Shuang-Shuang, QIU Xiao-Lang, *et al*. InGaAs quantum well based dual-wavelength external cavity surface emitting laser for wideband tunable mid-infrared difference frequency generation [J]. *Journal of Luminescence*, 2018: 663-667.
[14] Fan L, Fallahi M, Hader J, *et al*. Linearly polarized dual-wavelength vertical-external-cavity surface-emitting laser [J]. *Applied Physics Letters*, 2007, **90**(18).
[15] YU Qing-Nan, LI Xue, JIA Yan, *et al*. InGaAs-Based Well - Island Composite Quantum-Confined Structure with Superwide and Uniform Gain Distribution for Great Enhancement of Semiconductor Laser Performance [J]. *ACS Photonics*, 2018, **5**(12): 4896-4902.
[16] ZHENG Ming, YU Qing-Nan, Tai Han-Xu, *et al*. Experimental investigation of spontaneous emission characteristics of InGaAs-based indium-rich cluster-induced special quantum structure [J]. *Chinese Optics Letters*, 2020, **18**(5): 051403.
[17] MA Ming-Lei, Wu Jian, Ning Yong-Qiang, *et al*. Measurement of gain characteristics of semiconductor lasers by amplified spontaneous emissions from dual facets [J]. *Optics express*, 2013, **21**(8): 10335-10341.
[18] Yu Qing-Nan, Zheng Ming, Tai Han-Xu, *et al*. Quantum Confined Indium-Rich Cluster Lasers with Polarized Dual-Wavelength Output [J]. *ACS Photonics*, 2019, **6**(8): 1990-1995.
[19] TANIUCHI T, NAKANISHI H. Continuously tunable terahertz-wave generation in GaP crystal by collinear difference frequency mixing [J]. *Electronics Letters*, 2004, **40**(5): 327-328.